CLM - P 561

CLM - P 561

UKAEA

Preprint

SOFT X-RAY MEASUREMENTS OF THE IMPURITY DENSITY IN DITE

R D GILL
K B AXON
J W M PAUL
R PRENTICE

CULHAM LABORATORY
Abingdon Oxfordshire

1979

CLM-P 561

SOFT X-RAY MEASUREMENTS OF THE IMPURITY DENSITY IN DITE

R.D. Gill, K.B. Axon, J.W.M. Paul and R. Prentice

Culham Laboratory, Abingdon, Oxon, OX14 3DB, UK
(Euratom/UKAEA Fusion Association)

A B S T R A C T

We have measured the soft X-ray emission from the DITE tokamak for a wide range of different conditions. The coronal equilibrium model has been used to interpret the results and to show that plasma has been observed ranging from a nearly pure H plasma to one completely dominated by impurities. The effect on the impurities of the DITE bundle divertor and of gettering the torus walls have both been clearly established.

(Submitted for publication in Nuclear Fusion)

October 1978
KS

1. INTRODUCTION

The problem of plasma purity is of great importance for thermonuclear plasmas. It is therefore of considerable interest in present tokamaks to study impurity concentrations by measuring the absolute intensity of the soft X-ray continuum spectrum in the 1 - 5 keV range, and this has already been done for the ST [1] and TFR [2] tokamaks. In regions of the X-ray spectrum free from line radiation, the dominant source of X-rays is usually due to free-bound recombination radiation from impurity ions and the observed continuum radiation will exceed that expected for a pure H plasma by the X-ray anomaly factor, ζ. To interpret experimentally determined values of ζ it is necessary to be able to calculate the theoretical values, given the impurity concentration of the plasma and the main plasma parameters such as electron temperature and density. These calculations are outlined below in section 2 and can be found in more detail in references [1,2]. A vital feature of the calculation is a knowledge of the charge states of each impurity species and for the present results we have assumed that they can be calculated from the coronal equilibrium model.

The measurements described have all been carried out on the DITE tokamak (R = 1.17m, a = 0.27 m, B_ϕ = 1.0 - 2.8 T, I_G = 50 - 200 kA) and some of the results have been reported previously [3,4]. The details of the X-ray detection system are described in section 3 and the experimental results are in section 4.

2. SOURCES OF CONTINUOUS RADIATION

In a hot plasma at temperature, T_e, a continuous spectrum of X-rays will be emitted due to bremsstrahlung radiation from electron-ion collisions and also due to free-bound recombination radiation. If the plasma electron density is n_e, and the ion density n_z, then

the X-ray energy spectrum can be written [1] as:

$$\frac{dN}{dE} = \alpha\, n_e\, n_z \frac{e^{-E/T_e}}{E\sqrt{T_e}} \left\{ Z_a^{\,2}\, g_{ff} + Z^2\, g_{fb}\, \beta(Z) \right\} \text{cm}^{-3}.\text{s}^{-1}.\text{eV}^{-1} \qquad \ldots (1)$$

where

$$\beta(Z) = \frac{\xi}{\mu^3} \frac{\chi_\mu}{T_e} \exp\left(\frac{\chi_\mu}{T_e}\right) + \sum_{\nu=1}^{\infty} \frac{2\,\chi_H}{T_e} \frac{Z^2}{(\mu+\nu)^3} \exp\left[\frac{Z^2\,\chi_H}{(\mu+\nu)^2\, T_e}\right] \qquad \ldots (2)$$

$$\alpha = 9.6 \times 10^{-14}.$$

The ionic charge is Z, and Z_a is the atomic number; g_{ff} and g_{fb} are the free-free and free-bound Gaunt factors; the X-ray energy, E, and T_e are in units of eV as also are the ionization potential for H, χ_H, and χ_μ, the ionization potential of the atomic ground state. The use of the factor $Z_a^{\,2}$ in the first term of equation (1) is actually appropriate only for high electron energies where screening corrections are unimportant. However, the use of this factor for all energies will not produce large errors since the first term is usually substantially smaller than the second [1]. The first term of (2) represents recombination of the lowest unoccupied levels which have a common principal quantum number, μ. It is assumed that all these levels have the same ionization potential. ξ ($\leq 2\,\mu^2$) is the number of vacancies in the μ-shell of the atom before recombination has taken place. The second term of (2) represents the effects of recombination to states with higher principal quantum numbers and it has been assumed that their ionization energies can be accurately represented by $\chi_\lambda = Z^2\,\chi_H/\lambda^2$ with $\lambda = (\mu + \nu)$.

In practice there will be many different impurities in a plasma, each of which will be in several different charge states and the observed emission spectrum will then be represented by the sum:

$$\frac{dN}{dE} = n_e^{\,2}\, G(E, T_e) \sum_i \frac{n_{z_i}}{n_e} \left[Z_{a_i}^{\,2} + Z_i^{\,2}\, \beta(Z_i) \right] \qquad \ldots (3)$$

with

$$G(E,T_e) = 9.6 \times 10^{-14} \frac{e^{-E/T_e}}{E\sqrt{T_e}} \qquad \ldots (4)$$

and where we have assumed that the Gaunt factors are all unity. This is usually a good approximation within 20% [1] except for H where $g_{ff} = 0.5$. It then follows that the emission spectrum can be written as

$$\frac{dN}{dE} = n_e^2 \, G(E,T_e) \, \zeta \qquad \ldots (5)$$

which then defines the X-ray anomaly factor as the enhancement of the emission relative to that expected for free-free recombination from a pure H plasma with $g_{ff} = 1$.

In order to calculate ζ it is necessary first to evaluate $\beta(Z_i)$ for the different impurities in the plasma. Using the ionization potentials from reference [5] and equation (2) values of $\beta(Z_i)$ have been calculated for O, Fe and Mo. The latter values are shown in Fig. 1 where β is plotted as a function of T_e for various values of Z_i. It can be seen that β is a very sensitive function of electron temperature and this may lead to inaccuracies in the calculated values of ζ.

To proceed further it is necessary to know the values of the terms (n_{Z_i}/n_e) and these depend both on the absolute impurity concentration of a particular species and the relative distribution of each species amongst the different charge states. As a simplification we will assume that the coronal equilibrium model will apply and that all the ions of a particular species are in the most probable charge state (Z_i^*) determined by this model. The values of Z_i^* have been taken from the calculations of reference [6] in which the effects of both radiative recombination and dielectronic recombination were taken into account. The values of β for these most probable values are shown in Fig. 1 and we will use these values in the remainder of this paper.

An expression for ζ may now be written as

$$\zeta = \sum_i \frac{n_{z_i}^*}{n_e} (Z_{a_i}^2 + Z_i^{*2} \beta(Z_i^*)) = \sum_i \frac{Z_i^* n_{z_i}^*}{n_e} \zeta_m(Z_i^*) \quad \ldots (6)$$

where the summation is over the different plasma species only. It is clear that the values ζ_m represent the anomaly factors for plasma composed entirely of a particular impurity ion and these calculated values are plotted in Fig. 2 as a function of electron temperature. It is these curves which we will use to interpret the experimental measurements made on DITE. However, the limitation and approximate nature of the calculations should be clearly recognised. In particular, relatively minor changes in the coronal model estimates of Z_i^* could make large differences to ζ_m values due to the strong variation of β with Z_i^*.

If a plasma is composed of hydrogen and only one impurity species, then it is possible to relate ζ and the effective charge $Z_e = \Sigma n_{zi} Z_i^2 / \Sigma n_{z_i} Z_i$ giving

$$(Z_e - \gamma) = \frac{(\zeta - \gamma)}{\zeta_m(Z_i^*)/Z_i^*} \quad \ldots (7)$$

where $\gamma = n_H/n_e$ and is the ratio of the number of hydrogen atoms to the number of electrons. The factor $\zeta_m(Z_i^*)/Z_i^*$ has been plotted in Fig. 3 as a function of T_e for the main impurity ions and it can be seen that because the values do not differ too widely from each other it will sometimes be possible to extract a value of Z_e from a measurement of ζ without a detailed knowledge of the impurity concentrations. Usually $Z_e, \zeta >> 1$ and it will then be reasonable to set $\gamma = 0$ in equation (7).

3. EXPERIMENTAL EQUIPMENT

For this series of experiments we used an 160 eV resolution, Si(Li), ORTEC detector [7] together with a standard electronic system

and a multi-channel pulse height analysis system. The detector had an area of 12 mm^2 and its efficiency was 100% except at low energies (< 0.7 keV) where its efficiency was reduced by the presence of an 0.008 mm Be vacuum window and at high energies (> 30 keV) where the detector becomes transparent to the incident radiation. The spectra generated by this detector were recorded in the multi-channel analyser with care taken to ensure that none of the spectra was distorted by pile-up effects resulting from high count rates.

The detector viewed the DITE plasma radially through an evacuated tube which also contained two sets of apertures and foils separated by 1.2 m, one near the plasma and the other close to the detector. The apertures were adjusted to maintain a reasonable count rate in the detector and the foils were used to cut off unwanted parts of the low energy spectrum. The apertures had diameters in the range 0.3 to 6.5 mm and the foils were either Be of thickness 0.015 to 0.10 mm or Aℓ with thickness 0.01 to 0.09 mm. The energy calibration of the detector was checked with an <u>in situ</u> ^{55}Fe source.

A typical X-ray spectrum is shown in Fig. 4 and the effect of the low energy cut off can be clearly seen. The spectrum is smooth and featureless although in some spectra we observed a line at 2.45 $\pm$ 0.1 keV which we attributed to the L line of Mo (Fig. 5). Many spectra also showed enhanced emission in the E < 1.1 keV region and this was attributed to the L lines from Fe. No further line features were expected in this spectral region and so the regions away from the line radiation can be used with confidence to determine electron temperatures and X-ray anomaly factors.

The observed continuum spectrum is more complicated than that given by equation (5) since the observed emission occurs from plasma with varying density and temperature. The observed spectrum may be

calculated by integrating equation (5) over the line of sight

$$\frac{dN}{dE} = \int_{-a}^{+a} n_e^2(r)\ G(E,T_e(r))\ \zeta(r)\ dr \qquad \ldots (8)$$

where a is the limiter radius. This equation has been evaluated assuming that ζ is independent of radius which is reasonable since the main contribution to the integrand will be from a small volume near to r = 0. The profiles for n_e and T_e were taken from the ruby laser diagnostic measurements. However, the calculations showed that the spectrum was fairly insensitive to the detailed profiles but depended mainly on the peak electron temperature and density. It can be seen from Fig. 4 that the calculated spectrum provides a good fit to the experimental data, implying good agreement between the electron temperature determined by the laser and X-ray systems. We have found [8] over a wide range of conditions that these two quantities agree to within 10%.

In the measurements reported below we have assumed fixed profiles for n_e and T_e and used the microwave measurements to determine $\bar{n}_e$. T_e was sometimes taken from the laser measurements but more often from the slope of the X-ray energy spectrum.

4. EXPERIMENTAL RESULTS

In the first period of operation of DITE the discharge was initially dominated by low Z impurities but at a later date spectroscopic evidence showed that the low Z impurity concentration diminished, leaving discharges dominated by high Z materials - Mo from the limiter and Fe and other ions from the stainless steel torus walls [3,9]. This also resulted in the observation of hollow T_e profiles [10] which were attributed to radiation cooling of the plasma centre. The first set of measurements reported below (sub-sections 4.1 and 4.2) were taken during the period of metal domination but before the discovery of the hollow profiles.

Subsequently, the nature of the DITE discharges was substantially changed by gettering the torus walls with a layer of Ti [11]. This resulted in discharges with much higher densities and the measurements corresponding to these conditions are reported in sub-section 4.3.

4.1. Divertor Studies

The DITE bundle divertor and its mode of operation has already been described [3,9,12].

The present results were obtained with a gas current I_G = 50 kA, a toroidal field strength B_ϕ = 0.9 T giving discharges with q = 5.5 at the limiter. With the divertor switched off typical parameters were achieved of $\hat{T}_e$ = 300 eV, $\bar{n}_e = 5 \times 10^{12}$ cm^{-3} and ζ = 800. With the divertor on, it was found that ζ was reduced on average to about 150 with small changes in the other parameters (see Fig.6). The straightforward interpretation is that the overall plasma impurity level has been reduced by the divertor action by a factor of $\approx$ 5 and this compares well with the spectroscopic information which shows [9] that the divertor reduces the VUV emission from Mo, Fe, Cr and O by factors of 10, 3, 3 and 1.6 respectively.

As there are known to be several different impurities in the plasma it is not possible to extract the individual impurity densities from the X-ray measurements but instead maximum possible impurity densities can be calculated by assuming that a particular species is the only impurity. These maximum densities are calculated using the values of ζ_m shown in Fig. 2. With the divertor 'off' the measured value of ζ implies high Mo concentration with n_{Mo}/n_e = 3.0%. The other impurities do not have sufficiently high values of ζ_m to explain the observations. With the divertor 'on' the calculated impurity concentration falls to n_{Mo}/n_e = 0.4%. A noteable feature of the impurity densities is their very large magnitudes - with the divertor off the

measurements indicate that the plasma electrons are almost entirely derived from the impurity ions.

The value of Z_e may also be found from ζ using equation (7) and assuming $\gamma \sim 0$. If the two extreme values of $\bar{\zeta}_m/Z_i^*$ are taken from Fig. 3 then $Z_e = 8 \rightarrow 24$ with the divertor off and Z_e $1.5 \rightarrow 16$ when it is on. One therefore expects a considerable reduction in Z_e which is not fully reflected by the values from resistivity measurements of $Z_e = 2.9$ (Divertor 'off'), $Z_e = 1.9$ (Divertor 'on'). In some experiments [13], Z_e has remained constant despite a considerable reduction in ζ and in impurity VUV emission. Although we have no qualitative information, a possible explanation [1] of this observation would be the existence of a runaway current reducing the apparent plasma resistance. This would reduce the observed values of Z_e and mask changes in Z_e due to changes in plasma impurity level. This explanation is quite plausible in view of the low operating density of the 50 kA discharges used for the divertor operation.

4.2. Metal Dominated Discharges

A further set of discharges was investigated with $q \approx 4$ and $I_G = 100 - 200$ kA. A few of these discharges had very high ($\approx$ 2000) values for ζ and these cannot be interpreted using the coronal model as they exceed the maximum calculated values, ζ_m, by a factor of 2 or more. However, these large values do again point to the existence of discharges with very high impurity levels, probably Mo.

Other discharges had lower values of ζ and for the condition $B_\phi = 2.0$ T, $I_G = 150$ kA, $\hat{T}_e = 418$ eV and $\bar{n}_e = 1.6 \times 10^{13}$ cm^{-3} we measured $\zeta = 300$. The values of ζ_m of Fig. 2 then show that the plasma must be dominated by Mo impurities if we exclude the possibility of oxygen contamination on the general spectroscopic grounds referred to in

section 4.1. Values of $n_{Mo}/n_e = 1.1\%$ and $Z_e = 7.5$ are found, with the latter value larger than the experimentally determined $Z_e = 3.0$.

The values of the impurity concentration suggested by this analysis are extremely high and the effects of radiation loss from the plasma centre can then have a dominant influence on the plasma energy balance. The Ohmic power at the plasma centre is calculated to be $P_\Omega = 0.8$ W cm^{-3} compared with the calculated [14] radiated power $P_r = 1.4$ W cm^{-3}. Although we cannot have $P_r > P_\Omega$ as the discharges have a peaked T_e profile, this result clearly suggests that radiation loss from the plasma centre is the dominant loss mechanism.

In other discharges the discordance between P_r and P_Ω is more than a factor of 2, suggesting that we are generally over estimating the Mo concentration and this may indicate deficiences in our simple coronal model calculations. However, despite these difficulties, the measurements clearly indicate the existence of plasma heavily dominated by impurities.

4.3. High Density Discharges

The immediate effect of gettering the torus walls with Ti, together with the introduction of a continuous gas feed, was to allow machine operation at very much higher densities [11] (see Fig. 7). At the same time a very marked reduction in X-ray emission was observed from $\zeta \approx 800$ to $\zeta \approx 8$ and this effect is clearly shown by Figs. 6 and 7 where the experimentally determined values are plotted for discharges with $I_G = 50 - 200$ kA and $q = 3 - 5$. In the gettered discharges ζ decreases in part due to the increase in electron temperature and density; Fig. 2 shows that the values of ζ_m, and thus ζ, decrease as T_e increases. Despite this, the gettering clearly causes a reduction in impurity density by a factor of ≈ 10. Using the data from Fig. 2 maximum

impurity densities with the getters 'on' are: $n_o/n_e \leq 0.5\%$, $n_{Fe}/n_e \leq 0.4\%$, $n_{Mo}/n_e \leq 0.07\%$ where the estimate for Fe will also include contributions from the other components (eg Cr) of the stainless steel torus. The Z_e values extracted from the anomaly factors by assuming each impurity in turn were in the range $Z_e = 1.1 \rightarrow 2.7$ and were in good agreement with the values determined from the plasma resistance.

In these high density discharges, the effect of the divertor on the value of ζ was negligible, but as these discharges were already quite pure it was probably unreasonable to have expected any further improvement. The anomaly factor also showed that the injection of 200 kW of 30 keV H neutrals into the plasma made no substantial change to the impurity density. In contrast, the addition to the filling gas of a few per cent of Ne gave an increase to $\zeta = 84$.

4.4. Comparison With Other Measurements

Information about impurity concentrations in the DITE plasma has also been obtained from VUV measurements [15] and surface physics measurements [4] and so a comparison with the present results is possible. Unfortunately only limited comparisons can be made with the VUV work due to the small number of discharges in common with both sets of measurements. The impurity concentrations suggested by the VUV work are lower than our values. Using these values it is possible to calculate an anomaly factor, $\zeta = 50$, which is substantially smaller than the lowest value, $\zeta = 250$, measured for similar ungettered discharges. We have not been able to resolve this discrepancy in a satisfactory manner but more experimental data could help. However, the relative changes in ζ are well correlated with the changes in VUV emission for the divertor work (cf § 4.1).

The comparison with the surface physics results is more satisfactory.

In these experiments, measurements are made of the flux of metal atoms at the periphery of the plasma. 100 ms after the initiation of the discharge, it was found [4] that the metal fluxes in gettered and ungettered discharges were in the ratio 12:1.3. This is in excellent agreement with the reduction in impurity density by a factor of 10 deduced from the X-ray measurements. It would therefore appear that the impurity density at the plasma centre is strongly correlated with the atomic impurity flux at the plasma edge.

5. CONCLUSIONS

The principal conclusions of this paper are as follows:

(i) The measurement of the soft X-ray spectrum is a simple and valuable way to study tokamak relative impurity densities.

(ii) The DITE divertor has been shown to reduce the impurity density of an impure discharge by a factor of ≈ 5.

(iii) Gettering the torus walls produced discharges with higher electron densities and lowered the impurity density by a factor of 10.

(iv) Some discharges have been observed in DITE which were heavily contaminated with metal impurities.

(v) Comparisons of the soft X-ray impurity densities with those deduced from the radiative power balance, measurements of Z_e and VUV measurements suggest that the soft X-ray values are consistently on the high side. This suggests that the values of ζ_m may be too small and it would therefore be worthwhile to recalculate values of ζ_m using a more sophisticated model than that used in the present paper. It would be useful to include the correct Gaunt factors as calculated, for example, by Karzas and Latter [16] and to evaluate the contributions to ξ_m from different charge states separately rather than using the average value of the ionic charge Z_i^*. This has already been done in the calculations of ref [17].

The effects of diffusion of the charged ions could also be of importance as could deviations from coronal equilibrium. These latter factors would be difficult to incorporate into a calculation of ξ_m without extensive further information about the distribution of impurities and their charge states within the tokamak plasma.

6. ACKNOWLEDGEMENTS

We would like to thank Drs N.J. Peacock, S.J. Fielding, R.J. Bickerton and H.P. Summers for their many helpful comments on this work.

REFERENCES

[1] S. von Goeler, W. Stodiek, H. Fishman, S. Grebenshchikov and E. Hinnov, Nuclear Fusion 15, (1975) 301.

[2] Equipe TFR, Nuclear Fusion 17, (1977) 213.

[3] J.W.M. Paul, A.E. Costley, S.J. Fielding, M.J. Forrest, R.D. Gill, J. Hugill, G.M. McCracken, N.J. Peacock, P.E. Stott, 8th Europ. Conf. on Controlled Fusion and Plasma Physics, Prague 2 (1977) 49.

[4] G.M. McCracken, G. Dearnley, R.D. Gill, J. Hugill, J.W.M. Paul, B.A. Powell, P.E. Stott, J.F. Turner, J.E. Vince, paper contributed to the 3rd Int. Conf. on Plasma-Surface Interactions in Controlled Fusion Devices, Culham (1978).

[5] T.A. Carlson, C.W. Nestor, N. Wasserman and J.D. McDowell, Atomic Data 2 (1970) 63.

[6] C. Breton, C. de Michelis and M. Mattioli, EUR-CEA-FC-853.

[7] D.A. Gedcke, X-Ray Spectrometry, 1 (1972) 129.

[8] R. Prentice, CLM R-179, Culham Laboratory, UK (1978).

[9] J.W.M. Paul, K.B. Axon, J. Burt, A.D. Craig, S.K. Erents, J. Hugill, S.J. Fielding, R.D. Gill, D.J. Goodall, R.S. Hemsworth, M. Hobby, G.M. McCracken, A. Pospieszczyk, B.A. Powell, R. Prentice, G.W. Reid, P.E. Stott, D.D.R. Summers and C.M. Wilson, Plasma Physics and Controlled Nuclear Fusion Research, Berchtesgaden 2 (1976) 269.

[10] J. Hugill, S.J. Fielding, R.D. Gill, M. Hobby, G.M. McCracken, J.W.M. Paul, N.J. Peacock, B.A. Powell, R. Prentice, P.E. Stott 8th Europ. Conf. on Controlled Fusion and Plasma Physics, Prague 1 (1977) 39.

[11] S.J. Fielding, J. Hugill, G.M. McCracken, J.W.M. Paul, R. Prentice, P.E. Stott, Nuclear Fusion 17 (1977) 1382.

[12] P.E. Stott, C.M. Wilson and A. Gibson, Nuclear Fusion 17 (1977) 481, Nuclear Fusion 18 (1978) 475.

[13] S.J. Fielding, M. Hobby, J. Hugill, G.M. McCracken, J.W.M. Paul, N.J. Peacock, B.A. Powell, P.E. Stott 8th Europ. Conf. on Controlled Fusion and Plasma Physics, Prague, 1 (1977) 36.

[14] R.V. Jensen, D.E. Post, W.H. Grasberger, C.B. Tarter, W.A. Lokke, Nuclear Fusion 17 (1977) 1187.

[15] G.M. McCracken, D.H.J. Goodall, L.B. Bridwell, G. Dearnley, J.H. Shea, C.J. Sofield, J. Turner, N.J. Peacock, M.H. Hughes, H.P. Summers, M.G. Hobby, M.W.D. Mansfield and S.J. Fielding, paper IAEA/CN/37-N-5 contributed to the 7th Int. Conf. on Plasma Physics and Controlled Nuclear Fusion Research, Innsbruck (1978); M.G. Hobby, private communication.

[16] W.J. Karzas and R. Latter, Astrophys. J. Suppl. Series 6 (1961) 167.

[17] D.A. Marty, P. Smeulders and D. Lannois, EUR-CEA-FC-969 (1978).

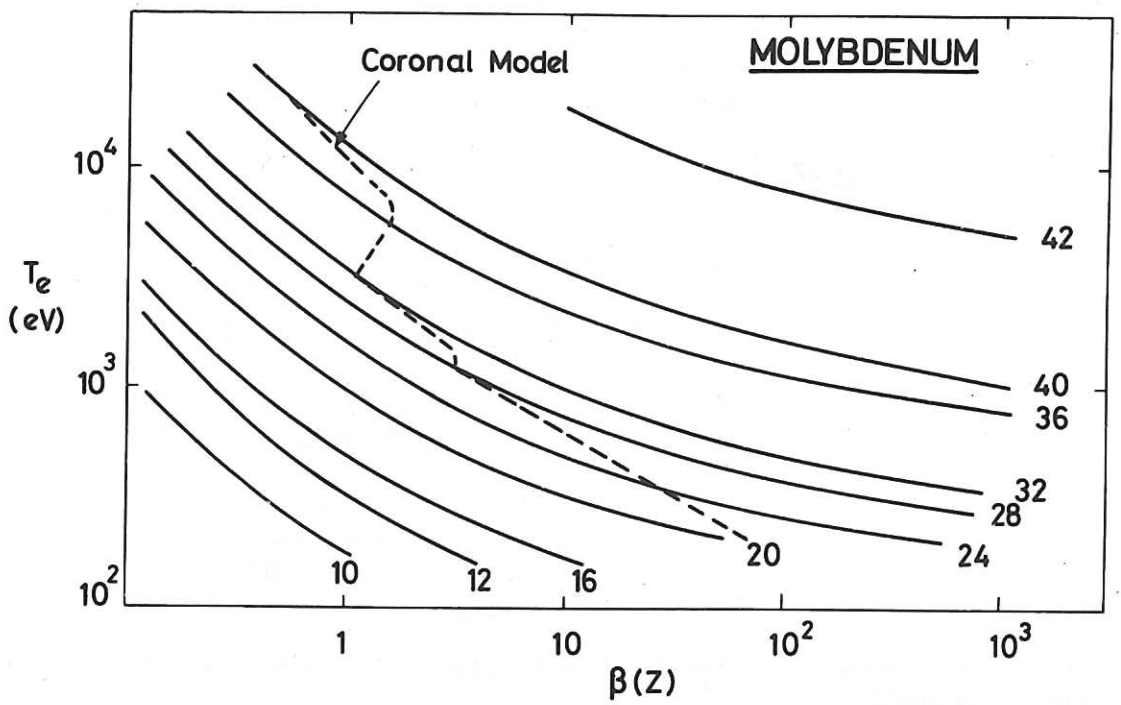

Fig.1 The quantity $\beta(Z)$ is plotted as a function of T_e for Mo. The broken line joins the most probable charge states given by the coronal equilibrium model and defines $\beta(Z_i^*)$.

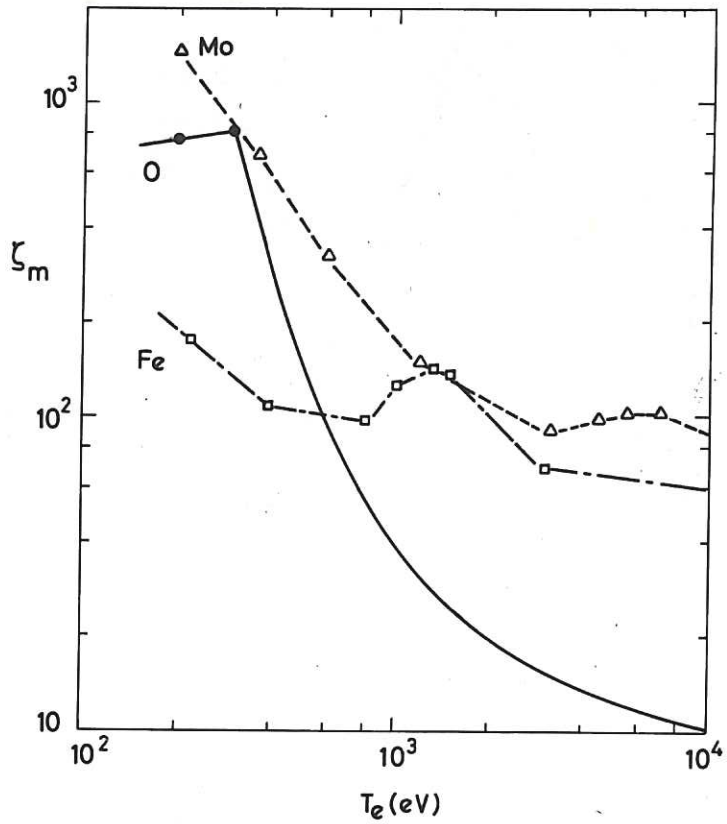

Fig.2 The maximum X-ray anomaly factors, ζ_m, are shown for 0, Fe and Mo. In each case, the calculated values assume that the plasma is entirely composed of one particular ion. Each point on the graph corresponds to a most probable charge, Z_i^*.

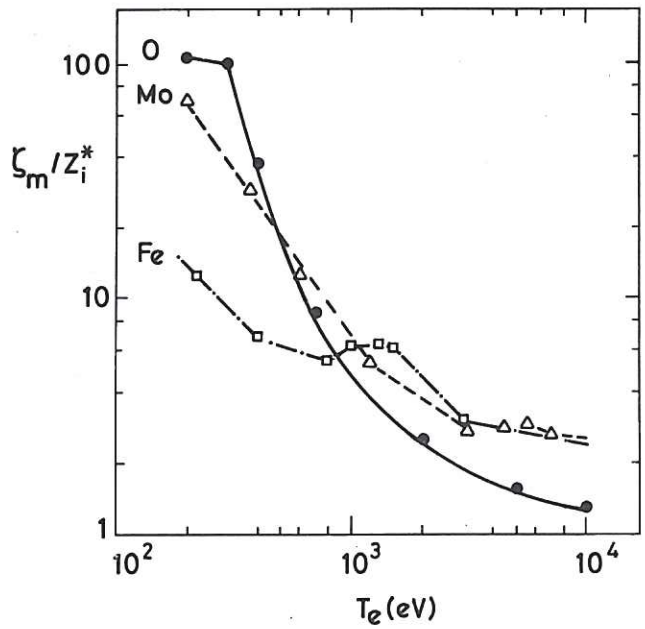

Fig.3 ζ_m^*/Z_i^* is plotted as a function of T_e for 0, Fe and Mo. This quantity is used to deduce Z_e from measured values of ζ.

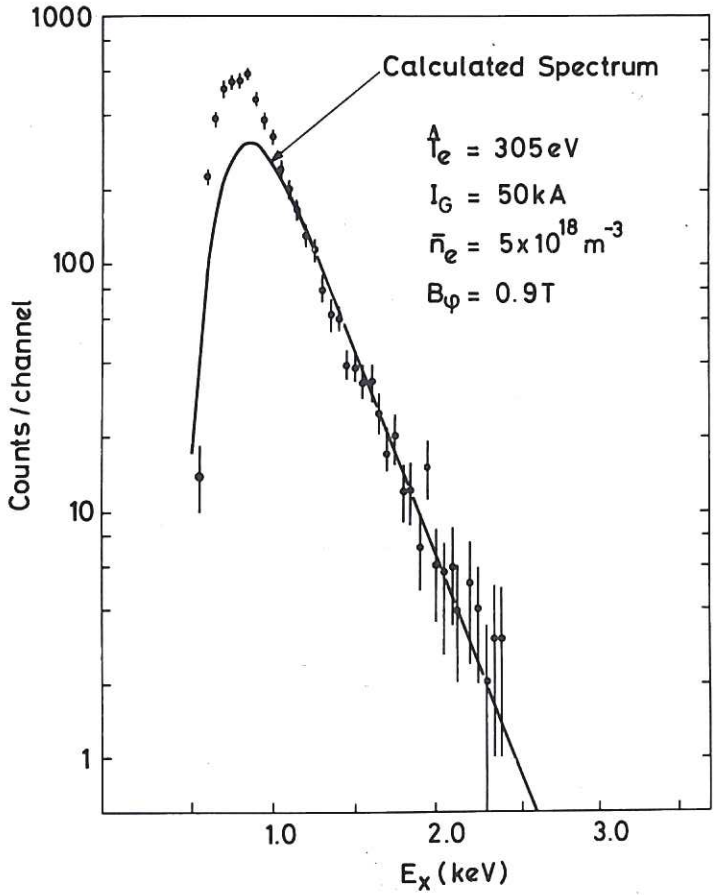

Fig.4 An X-ray spectrum is shown together with a fit to the spectrum calculated to include the effects of the plasma profile and the absorption at low energy due to the presence of a thin Be foil 0·008 mm thick. The ordinate is proportional to dN/de.

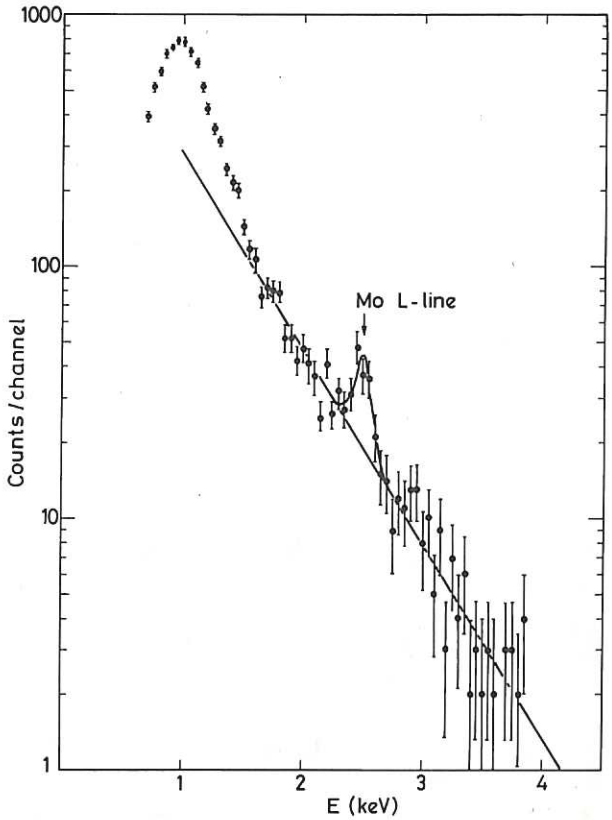

Fig.5 This X-ray spectrum shows the Mo L-line at an energy of 2·45 keV. The straight line fit to the upper part of the spectrum shows that this feature is well above the background continuum. The spectrum was taken using a Be absorber of 0·008 mm.

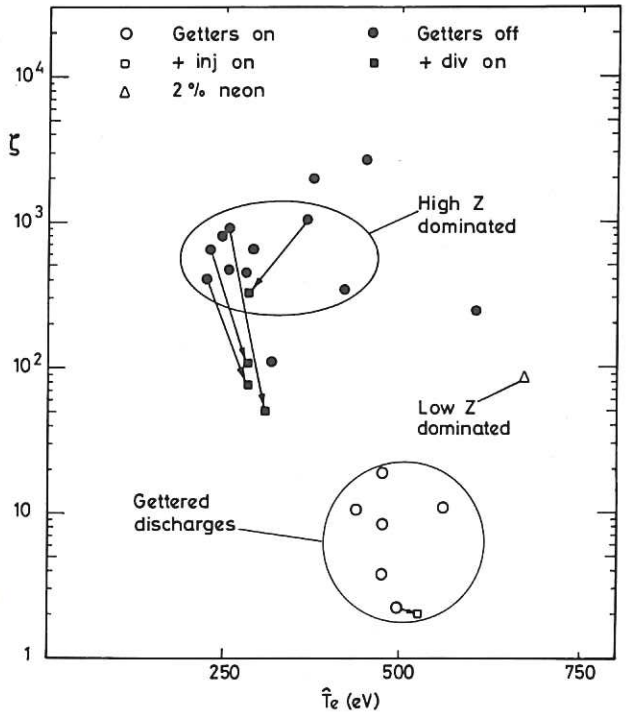

Fig.6 The measured values of ζ are plotted against T_e. The effect of the divertor upon impurity concentration is shown by the pairs of full points connected by arrows. The effect of gettering in reducing impurity concentration can also be clearly seen. The getters were 'on' for all the open points on the graph.

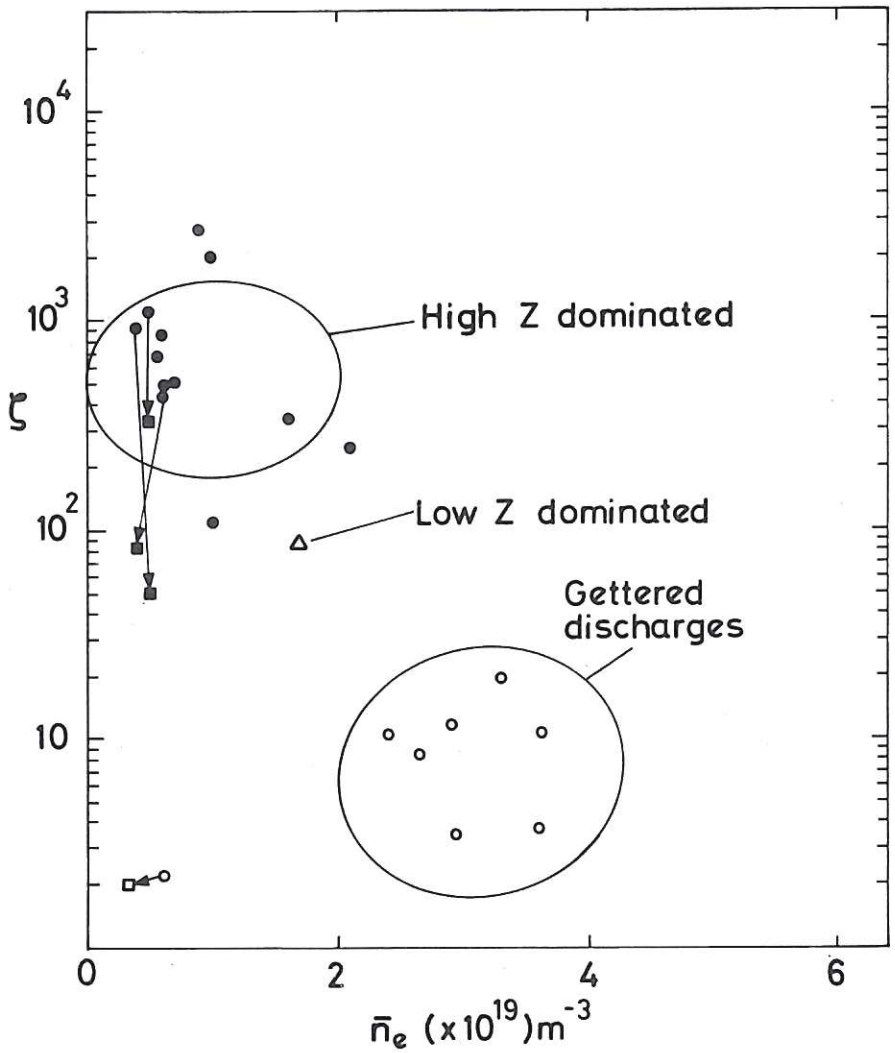

Fig.7 The measured values of ζ are plotted against T_e. The trend to lower ζ-values at high density is clearly visible especially for the gettered discharges. The legend on Fig.6 describes the different points.